Electrophotoluminescence in Semiconductors

Konrad Colbow

Bell Telephone Laboratories, Murray Hill, New Jersey

Four electric-field effects on photoluminescence have been observed in the low-temperature green-edge emission in GaP. These are the Gudden-Pohl effect, field quenching, field enhancement, and field broadening of the emission band. From independent evidence the edge emission is known to result from the reaction between electrons bound to donor impurities (sulfur) and holes bound to acceptor impurities (silicon). The data are explained on a semiquantitative basis, in terms of these donor-acceptor pairs, using a refined version of a previously described theoretical model in which it is not necessary to invoke trapping or de-trapping from traps of known or unknown origin. The theoretical model employs hydrogenic impurity wave functions, and as before leads to the observed nonexponential time decay of the photoluminescence. The electric-field effects are taken care of by considering the action of the field on the impurity wave functions, using a WKB approximation.

I. INTRODUCTION

IN electrophotoluminescence one studies the changes in the photoluminescence, produced by an applied electric field which is too small to cause appreciable electroluminescence. Three basic effects have been distinguished in the past. First there is the Gudden-Pohl effect,[1] which consists of a transient increase in light output every time an electric field is changed in direction, turned on, or switched off. The other two effects are quenching, and enhancement of the photoluminescence by an electric field. The former is by far more common, and was first investigated by Coustal[2] and Déchêne,[3] while field enhancement was first observed by Destriau[4] in 1954. Since then all three effects have been studied by a large number of workers both for electroluminescent and nonelectroluminescent phosphors, notably in such II-VI compounds as $(Zn, Cd)S:Cu$,[5] $ZnS:Mn$, $Cl \neq C1$,[6] and $ZnS:Cu$, Al.[6] A review of the subject of electrophotoluminescence together with a more complete list of references to previous work may be found in an article by Ivey.[7]

Even a qualitative understanding of the subject is at present rather incomplete, and for many aspects contradictory opinions are held. The Gudden-Pohl light flashes are attributed to the effect of the field on electrons in traps of unknown origin. According to Ivey,[7] the most obvious mechanism for the Gudden-Pohl effect is that the field liberates trapped electrons by a tunneling process or by thermal liberation over a potential barrier lowered by the field. However, Curie[8] believes that the traps are emptied by the impact of electrons accelerated in the conduction band by the

field. Field quenching is usually believed to result from field-induced nonradiating transitions through traps of unknown origin.[9] Field enhancement is either attributed to a kinetic effect resulting from the competition of several simultaneous processes,[10] or to "radiation-controlled electroluminescence"[11,12] resulting from acceleration of electrons introduced into the conduction band by the exciting radiation. Thus, the three basic electrophotoluminescent effects are believed to be essentially unrelated.

All three effects have been seen in the low-temperature green-edge emission in gallium phosphide, and it will be shown in this paper that, at least for GaP, they are apparently closely related. The part of the edge emission that was investigated is believed to result from the reaction of a bound electron with a bound hole and will hereafter be referred to as pair band. Several independent pieces of evidence for this mechanism have been obtained,[13,14] and more will be presented in this paper.

II. EXPERIMENTAL

Doped and intentionally undoped n-type crystals of GaP were grown from gallium solution. In all cases the predominant impurities were sulfur donors partially compensated by silicon acceptors. The donor and acceptor concentrations (N_D, N_A) and the donor binding

[1] B. Gudden and R. W. Pohl, Z. Physik **2**, 192 (1920).
[2] R. Coustal, Compt. Rend. **198**, 1403, 1596 (1934).
[3] G. Déchêne, Compt. Rend. **201**, 139 (1935); **205**, 850 (1937); J. Phys. Radium **9**, 109 (1938).
[4] M. Destriau, Compt. Rend. **238**, 2298 (1954).
[5] K. W. Olson and G. C. Danielson, Phys. Rev. **92**, 1323 (1953).
[6] H. Gobrecht, H. E. Gumlich, H. Nelkowski, and D. Langer, Z. Physik **149**, 504 (1957).
[7] H. F. Ivey, *Advances in Electronics and Electron Physics*, edited by L. Marton (Academic Press Inc., New York, 1963), Suppl. 1.
[8] D. Curie, J. Phys. Radium **13**, 317 (1952); **14**, 135, 510, 672 (1953); J. Mattler and D. Curie, Compt. Rend. **230**, 1086 (1950).

[9] F. Matossi, Phys. Rev. **94**, 1151 (1954); **98**, 434 (1955); **101**, 1835 (1956); Electrochem. Soc. **103**, 122, 662 (1956).
[10] M. Schon, Tech. Wiss. Abhandl. Osram-Ges. **6**, 49 (1953); Physica **20**, 430 (1954); H. F. Ivey, *Solid-State Physics in Electronics and Telecommunications*, edited by M. Désirant and J. L. Michiels (Academic Press Inc., New York, 1960), Vol. 4, p. 611; D. Curie, *Progress in Semiconductors*, edited by A. F. Gibson, P. Aigrain, and R. E. Burgess (John Wiley & Sons, Inc., New York, 1957), Vol. 2, p. 249.
[11] D. A. Cusano and F. W. Williams, J. Phys. Radium **17**, 742 (1956).
[12] W. A. Thornton, *Solid-State Physics in Electronics and Telecommunications*, edited by M. Désirant and J. L. Michiels (Academic Press Inc., New York, 1960), Vol. 4, p. 658.
[13] D. G. Thomas, J. J. Hopfield, and K. Colbow, Proceedings of the International Conference on the Physics of Semiconductors, Paris, 1964 (to be published).
[14] J. J. Hopfield, D. G. Thomas, and M. Gershenzon, Phys. Rev. Letters **10**, 162 (1963); D. G. Thomas, M. Gershenzon, and F. A. Trumbore, Phys. Rev. **133**, A269 (1964).

energy (E_D) were determined by Hall measurements made by Montgomery. From spectroscopic identification[14] E_A+E_D was determined (see Sec. III), and thus both the donor and acceptor binding energies are experimentally known. Several different experiments were performed on several samples, which in all cases were immersed in liquid helium during the experiment.

(1) The crystals were excited by a brief (3–4 μsec) flash of 3000- to 4000-Å light from a FX 12 xenon flash tube. The luminescence from the crystal was detected by means of a photomultiplier and followed on an oscilloscope as a function of time after excitation in the absence and presence of an applied electric field. Light emission other than the pair-band luminescence, such as bound exciton emission,[15] was excluded by means of Corning filters. However, such light did not interfere with the measurements in any case, since it decays much faster (in less than 1 μsec) than the pair-band radiation.

(2) The 3000- to 4000-Å light from a dc-operated HB-200 mercury arc was chopped by a sector of a rotating disk, and focused on the crystal. The resulting luminescence during the no-excitation interval was chopped again at the same frequency, but with a variable phase shift, dispersed by a spectrometer, detected by a photomultiplier, and displayed on an x-y recorder. By changing the chopping frequency, and/or the phase shift, photoluminescent spectra were taken at various times after excitation, with and without the applied electric field. The detailed experimental setup will be discussed elsewhere.[16]

Application of the electric field: The crystals were mounted on glass backing between condenser plates 2 mm apart. Neither side of the crystal touched the plates. The arrangement was essentially the same as that described by Thomas and Hopfield.[17] The crystal dimensions were about 1.7×1.0×0.08 mm, with the longest dimension perpendicular to the plates. The large ratio of the crystal dimensions perpendicular and parallel to the condenser plates ensures that the electric field inside the crystal is equal to the applied field[17] (voltage difference between condenser plates divided by plate separation), provided that electrostatic shielding due to the crystal conductivity is eliminated. Since the crystals are photoconductive, this requires the application of an alternating square-wave voltage to the plates, with a time interval less than the effective dielectric relaxation time.

III. THEORY

In the absence of an electric field, the energy of light emission $E(r)$, which results when a bound electron reacts with a bound hole, is given by

$$E(r) = E_{gap} - (E_A + E_D) + e^2/\epsilon r, \qquad (1)$$

provided the electron-hole separation r is large compared to the radii of the donor and acceptor states.[14] E_{gap} is the band-gap energy, E_A and E_D are the acceptor and donor binding energies, respectively, e is the electronic charge, and ϵ the static dielectric constant.

Since the donors and acceptors must fall on lattice sites, r can only have certain discrete values. Thus, one obtains a line spectrum for small r, and through the identification of definite values of r, and Eq. (1) it is possible to determine E_A+E_D. For larger values of r (50 to 150 Å), the emission merges into the continuous pair band under investigation.

For definiteness, and in agreement with the present experimental situation, it is assumed that the donors are in excess. An acceptor atom is then regarded as being surrounded by a random array of donors, and being independent of other acceptors. The initial flash of light is supposed to create sufficient holes and electrons to neutralize all the acceptors and donors in the excited volume. It is further assumed that after the flash there is no redistribution of the electrons and holes through thermal detrapping, or tunneling. This assumption seems to be justified, since the luminescence is nearly independent of temperature below 20°K.

Calculation of Decay of Total Radiated Light (No Applied Field)

The reaction of a bound hole with a bound electron will be treated as a kind of annihilation process, resulting in the emission of light. The optical matrix element is

$$M = \int \psi_f P \psi_i d\tau, \qquad (2)$$

where ψ_f is the final- and ψ_i the initial-state wave function of the electron. P is an operator, and the integration is performed over all space.

In the effective-mass formalism for shallow donor and acceptor states,[18] the final- and initial-state wave functions are the Bloch-function-modulated effective-mass-envelope wave functions. These satisfy the hydrogen-like effective-mass Schrödinger equation for an acceptor and donor state, respectively. In particular, for the ground state of an isolated acceptor and donor, the envelope wave functions are assumed to be the hydrogenic 1s wave functions.

$$\psi_h(1s) = A_h e^{-r_h/a_h},$$
$$\psi_e(1s) = A_e e^{-r_e/a_e}. \qquad (3)$$

Here A_e, A_h are constants; r_e and r_h are distances whose origin is the donor and acceptor site, respectively. In a hydrogenic approximation the effective Bohr radii a_e, a_h may be obtained from the experimentally determined values for the donor and acceptor binding

[15] D. G. Thomas, M. Gershenzon, and J. J. Hopfield, Phys. Rev. **131**, 2397 (1963).

[16] D. E. Thomas and K. Colbow (to be published).

[17] D. G. Thomas and J. J. Hopfield, Phys. Rev. **124**, 657 (1961).

[18] W. Kohn, *Solid-State Physics*, edited by F. Seitz and D. Turnbull (Academic Press Inc., New York, 1957), Vol. 5, p. 257.

energies E_i, using the hydrogenic energy relation

$$E_i = e^2/2\epsilon a_i. \tag{4}$$

When band-to-band transitions between the valence- and conduction-band extrema are allowed, Eq. (2) gives to a good approximation a constant times the overlap integral[19]

$$S = \int \psi_e \psi_h d\tau. \tag{5}$$

If band-to-band transitions are not allowed, as in GaP, the situation is more complicated. However, Eq. (2) will still be given to a good approximation by a constant times the overlap integral, provided one of the wave functions ψ_e, ψ_h decays much faster than the other. A detailed proof of this is given in Appendix I. In the present situation $a_h > a_e$, and hence the overlap integral S has a pronounced maximum at the donor site for all donor-acceptor separations R. Actually, the screened Coulomb interaction between the hole and the donor site will tend to push this maximum slightly toward the acceptor site; however, this shift will be neglected, since we are at present only interested in Eq. (2) for donor-acceptor separations which are large compared to the electron Bohr radius. Thus with these approximations the electron-hole reaction rate will be a constant times the squared overlap.

$$W(R) = CS^2(R). \tag{6}$$

The value of C is not easily calculated and will be left as an experimental parameter.

If the donor site is at the origin and the acceptor site has the Cartesian coordinates $(0,0,R)$, the hole wave function may be approximated near the origin by writing in Eq. (3) for $r \ll R$

$$r_h = [x^2 + y^2 + (z-R)^2]^{1/2} \approx R - z.$$

Since the overlap integral has a maximum near the donor site, it is thus immediately obvious from Eqs. (3), (5), and (6), that the reaction rate in the absence of an electric field is approximately given by

$$W(R) = C'e^{-2R/a_h}, \tag{7}$$

for $a_h > a_e$, $R \gg a_h$. The proportionality constant C' will be left undetermined.

The total light as a function of time using $W(R)$ is obtained by the following treatment given in Ref. 13. For an isolated pair of separation R, the normalized probability that the acceptor still has a hole on it after time t is

$$Q(R,t) = e^{-W(R)t}. \tag{8}$$

Because the transition rate for the disappearance of the hole by reaction with different donor electrons is addi-

[19] J. Shaffer and F. Williams, Proceedings of the International Conference on the Physics of Semiconductors, Paris, 1964 (to be published).

tive, the probability that an acceptor is still neutral after time t is

$$Q(t) = \exp\{-[\sum_i W(r_i)]t\} = \prod_i \exp[-W(r_i)t], \tag{9}$$

where the summation or product is over all donors in the crystal. For a random distribution, the probability of occurrence of a donor i a distance r from the acceptor is

$$P_i(r) = 4\pi r^2 \Big/ \left(\frac{4\pi}{3} r_0^3\right). \tag{10}$$

For the present calculation, the acceptor can be taken as the center of a spherical sample of radius r_0. Using Eqs. (9), (10), and the mathematical relation

$$\lim_{x \to \infty} [1 + (1/x)]^x = e,$$

one obtains for the average decay of neutral acceptors

$$Q(t) = N_A \exp\left\{N_D \int_0^\infty [e^{-W(r)t} - 1]4\pi r^2 dr\right\}. \tag{11}$$

Here N_A and N_D are the acceptor and donor concentrations per unit volume, and it was assumed that the sample is large enough to contain many donors. The intensity of the emitted light at time t is then given by

$$I(t) = -dQ/dt = 4\pi N_D Q(t) \int_0^\infty W(r)e^{-W(r)t} r^2 dr. \tag{12}$$

IV. THE EFFECTS OF AN APPLIED ELECTRIC FIELD

An applied electric field may be expected to have two fundamentally different types of effect. The first concerns the ground state of the system, that is the acceptor-donor pair after hole-electron reaction, while the second effect involves a distortion of the hole and electron wave functions by the applied field and thus a change in the hole-electron reaction rate $W(R)$.

A. The Effect of an Electric Field on the Ground State

The excited state of a "pair system" consists of a neutral acceptor and a neutral donor. After hole-electron reaction, the ground state of the system consists of an ionized acceptor and an ionized donor distant R apart. These constitute a dipole which in the presence of an applied electric field has a dipole energy associated with it, given by

$$\Delta E = eFR \cos\theta. \tag{13}$$

Here F is the internal electric field resulting from the applied field, e is the electronic charge, and θ is the angle the field direction makes with the dipole axis. This energy has to be added to Eq. (1) for the photon energy

from a particular hole-electron pair in the presence of an applied field. Averaging Eq. (13) over all θ from 0 to $\pi/2$, one may then expect the bandwidth from pair emission to increase by an amount of the order of

$$\langle |\Delta E|\rangle \approx \tfrac{1}{2}eFR, \tag{14}$$

provided the radiation is mainly caused by those pairs whose reaction rate is increased by the field, rather than decreased.

B. The Effect of an Electric Field on the Hole-Electron Reaction Rate

In the presence of an applied electric field the wave functions Eq. (3) become perturbed. However, usual perturbation theory will not readily give the proper wave functions at large distances, since many terms need to be considered, even for moderate fields like 4000 V cm^{-1}. While the ground-state wave-function perturbation at small distances is represented mainly in terms of the lowest excited states, the effect of higher excited states becomes important at large enough distances from the origin.

Thus it will be necessary to go directly to the Schrödinger equation which the envelope function satisfies in the presence of an applied field, and obtain the wave function of the WKB approximation. On account of its smaller Bohr radius one may neglect in first approximation the disturbance produced by the electric field on the donor-state wave function. This becomes especially clear when one remembers from the no-field situation that the overlap comes mainly from near the donor site, and one is thus only interested in the electron wave function for short distances.

For an isolated acceptor in an electric field F pointing along the negative z direction, the acceptor-state envelope wave function must satisfy the effective-mass Schrödinger equation

$$\left\{\nabla_h{}^2+\frac{2m^*}{\hbar^2}\left(E+\frac{e^2}{\epsilon r_h}-eFz_h\right)\right\}\psi_h(r_h)=0. \tag{15}$$

Here m^* is the light hole mass, ϵ the dielectric constant, and e the electronic charge. The subscript h on ∇, r, and z calls attention to the fact that the origin is the acceptor site.

Let us take the hole Bohr radius (a_h) as defined by Eq. (4) as unit of distance, twice the acceptor binding energy $2E_A$ as unit of energy, and $e\epsilon^{-1/2}$ as unit of charge. Further, let us set m^* and $\hbar$ equal to unity. The Schrödinger equation may then be written in the form

$$\{\tfrac{1}{2}\nabla_h{}^2+E+r_h{}^{-1}-F'z_h\}\psi_h=0, \tag{16}$$

where $F'=(eFa_h/2E_A)$.

Introducing parabolic coordinates

$$\xi=r_h+z_h, \quad \eta=r_h-z_h, \quad \varphi=\arctan(y/x), \tag{17}$$

Eq. (16) may be separated by the assumption

$$\psi_h=(\xi\eta)^{-1/2}u_1(\xi)u_2(\eta)e^{im\varphi}. \tag{18}$$

u_1 and u_2 both satisfy the differential equation

$$u''(x)+y(x)u(x)=0, \tag{19}$$

where

$$y(\xi)=E/2+Z_1/\xi-F\xi/4-(m^2-1)\xi^{-2},$$
$$y(\eta)=E/2+Z_2/\eta+F\eta/4-(m^2-1)\eta^{-2}, \quad Z_1+Z_2=1. \tag{20}$$

Between the two classical turning points x_1 and x_2, the WKB approximation gives for Eq. (19) the solution (see Ref. 20)

$$u=|y|^{-1/4}\cos\left(\int_{x_1}^{x}|y|^{1/2}dx-\frac{\pi}{4}\right). \tag{21}$$

Outside the far classical turning point x_2, the WKB solution is[20]

$$u=\tfrac{1}{2}|y|^{-1/4}\exp\left\{-\int_{x_2}^{x}|y|^{1/2}dx\right\}. \tag{22}$$

Since we shall assume that the donor is at the origin and the acceptor site has the Cartesian coordinates $(0,0,R)$, Eq. (17) leads to

$$\xi=[x^2+y^2+(z-R)^2]^{1/2}+(z-R),$$
$$\eta=[x^2+y^2+(z-R)^2]^{1/2}-(z-R). \tag{23}$$

Under the assumption that $r\ll R$, expansion of the square roots leads to

$$\xi=r^2/2R, \quad \eta=2R. \tag{24}$$

Thus, near the donor site $u_1(\xi)$ has the oscillatory form given by Eq. (21), while $u_2(\eta)$ exhibits the exponential decay given by Eq. (22), provided $F'\eta$ stays small enough that $y(\eta)$ does not become positive again.

For the ground state one has approximately $E=-\tfrac{1}{2}$ in units of $2E_A$, since a field of 8000 V cm^{-1} will not change the ground-state energy by more than about 0.6%. Also, $m=0$ and $Z_1=Z_2=\tfrac{1}{2}$ (see Ref. 20). Thus Eq. (20) simplifies to

$$y(\xi)=-1/4+1/2\xi-F'\xi+\xi^{-2},$$
$$y(\eta)=-1/4+1/2\eta+F'\eta+\eta^{-2}. \tag{25}$$

For small $|\xi|$, the ξ^{-2} term in $y(\xi)$ dominates. Replacing the cosine in Eq. (21) by its average value, and making use of Eq. (24) one thus obtains

$$u_1(\xi)=\tfrac{1}{2}|y(\xi)|^{-1/4}\approx(2R)^{-1/2}(r/2). \tag{26}$$

Substituting from Eqs. (24), (25), and (26) into Eq. (18), the ground-state hole wave function near the donor site has the form

$$\psi_h=AR^{-1/2}|1-8F'R|^{-1/4}e^{-\alpha/2} \tag{27}$$

[20] H. A. Bethe and E. E. Salpeter, *Handbuch der Physik*, edited by S. Flügge (Springer-Verlag, Berlin, 1957), Vol. 35, p. 88.

for

$$R \gg 1.$$

A is a constant, and

$$\alpha(F',R) = \int_{\eta_2}^{2R} \left(1 - \frac{2}{\eta} - \frac{4}{\eta^2} - 4F'\eta\right)^{1/2} d\eta. \quad (28)$$

Since donor-acceptor interactions have been neglected, the donor-state wave function is independent of R. Because of its smaller radius it is to a good approximation also independent of F, as discussed previously. Thus it is immediately obvious that the electron-hole reaction rate, being proportional to the squared overlap, is given by

$$W_F(R) = (D/R)|1 - 8F'R|^{-1/2}e^{-\alpha}. \quad (29)$$

The proportionality constant D is hard to calculate and will be left as an experimental parameter.

The classical turning point η_2 is obtained by setting the integrand in Eq. (28) equal to zero. Expansion for small fields results in

$$\eta_2 = 3.24(1 + 1.30F') \quad \text{for} \quad 1.3F' \ll 1. \quad (30)$$

Since the integrand in Eq. (28) vanishes at η_2, most of the contribution to $\alpha(F',R)$ comes from $\eta \gg \eta_2$, where the η^{-2} term may be neglected. Under the assumption that

$$(2/\eta + 4F'\eta) \ll 1, \quad (31)$$

the square roots in Eqs. (28) and (29) may be expanded. Keeping terms to first order in η^{-1} and $F'\eta$, one finds from Eq. (28)

$$\alpha = \int_{\eta_2}^{2R} \{1 - \eta^{-1} - 2F'\eta\} d\eta,$$

$$= 2R - \eta_2 - \ln(2R/\eta_2) - F'(4R^2 - \eta_2^2). \quad (32)$$

Substituting from Eqs. (30) and (32) into Eq. (29), and incorporating any multiplying constants into the constant D, one obtains for the electron-hole reaction rate approximately

$$W_F = D(1 + 4F'R)e^{-2R + 4F'R^2}, \quad (33)$$

for

$$a_h > a_e, \quad R \gg 1, \quad \text{and} \quad 8F'R \ll 1.$$

For the maximum field used, namely 8000 V cm^{-1}, $F' = 0.0113$ for $E_A = 0.05$ eV and $a_h = 14.1$ Å. Thus for $R \approx 10$, the limit of applicability of Eq. (33) is being reached.

For zero field Eq. (33) reduces of course to the same expression as Eq. (7), remembering that in Eq. (33) R is in units of a_h.

It follows from Eq. (33) that if the field direction is opposite to the donor-acceptor axis, the electron-hole reaction rate is increased, while the rate is decreased if the donor-acceptor axis points in the field direction.

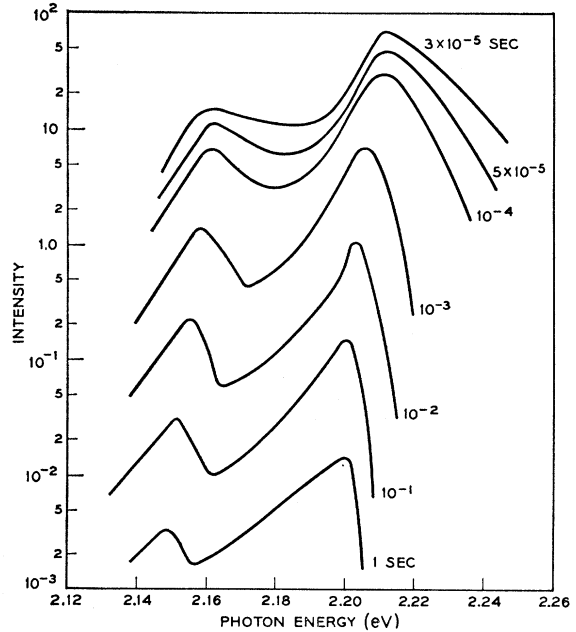If the axis for a given pair makes an angle θ with

FIG. 1. Experimental curves for spectra taken at various times after photoexcitation with crystal No. 2 at 1.6°K (Fig. 4 of Ref. 13).

the field direction, F' in Eq. (33) should be replaced by $F' \cos \theta$. To compare the theory with experiment it thus remains to average $W_{F \cos\theta}(R)$ over all angles the pair axes can make with the field direction. This average is
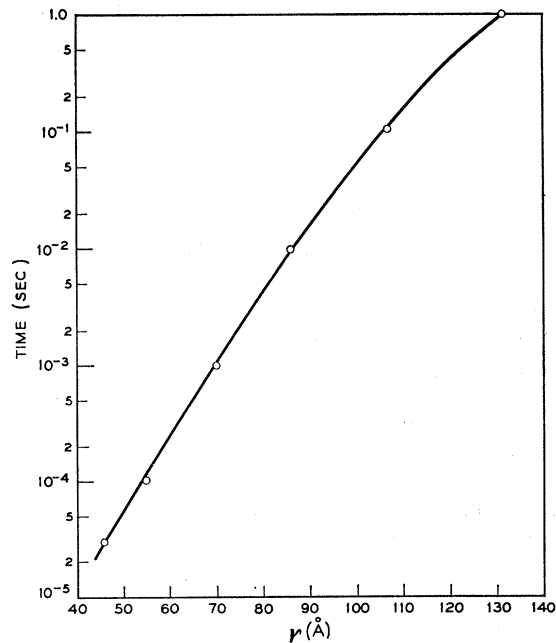

FIG. 2. Time of light emission after photoexcitation versus calculated mean electron-hole separation responsible for this light.

given by

$$\langle W_F \rangle = \frac{1}{2} \int_{-\pi/2}^{\pi/2} (W_{F\ \cos\theta}) \sin\theta d\theta,$$

$$= (C/2)e^{-2R} \int_{-1}^{1} (1+bx)e^{ax}dx,$$

$$= (C/2a)e^{-2R}\{(1+b-b/a)e^a - (1-b-b/a)e^{-a}\},$$

(34)

where

$$a \equiv 4F'R^2, \quad \text{and} \quad b \equiv 4F'R.$$

Thus the ratio of the reaction rate with and without an applied electric field is given by

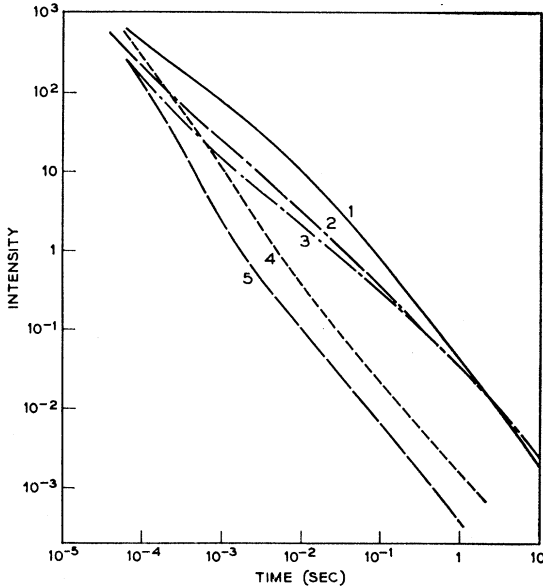$$\langle W_F \rangle / W_0 = (1/2a)\{e^a(1+b-b/a) - e^{-a}(1-b-b/a)\}, \quad (35)$$

FIG. 3. Experimental decay curves of the pair-band luminescence versus time after photoexcitation. The numbers on the curve refer to the crystals as marked in Table I.

and the increase of reaction rate with field is given by

$$\langle \Delta W \rangle = (C/2a)e^{-2R}\{e^a(1+b-b/a) - e^{-a}(1-b-b/a) - 2a\}. \quad (36)$$

V. EXPERIMENTAL DATA AND CALCULATIONS

A. Photoluminescence (No Applied Field)

Figure 1 is a reproduction of Fig. 4 in Ref. 13, and shows the spectrum of the low-temperature edge emission in GaP at various times after photoexcitation. Far-separated pairs decay slower and occur at lower energies. However, even for large separations where the spread in photon energy due to a spread in separation is small, since the Coulomb term in Eq. (1) is small, the

TABLE I. Impurity concentrations and relative dc brightness.

Crystal GaP, No.	N_D (sulfur)	N_A (silicon)	Relative dc brightness
1	2.0×10^{17}	1.0×10^{17}	100
2	2.4×10^{17}	5.0×10^{16}	67.4
3	1.0×10^{18}	1.2×10^{17}	45.0
4	1.3×10^{18}	1.0×10^{17}	14.4
5	4.2×10^{18}	2.5×10^{17}	3.6

pair band is not very sharp. This has been attributed to phonon cooperation,[13] but may also partly be caused by local-field fluctuations due to ionized impurities. The resolved smaller peak at lower energy is believed to be the LO phonon replica of the main peak, and it is apparent that acoustic phonons cooperate as well. This introduces some uncertainty into the plot of Fig. 2, where the mean electron-hole separation responsible for the emitted light has been shown as a function of the time after photoexcitation. The values of r were obtained by using Eq. (1), with $E(r)$ determined from the peak positions of Fig. 1, $E_{\rm gap} - (E_A + E_D) = 2.1857$ eV,[14]
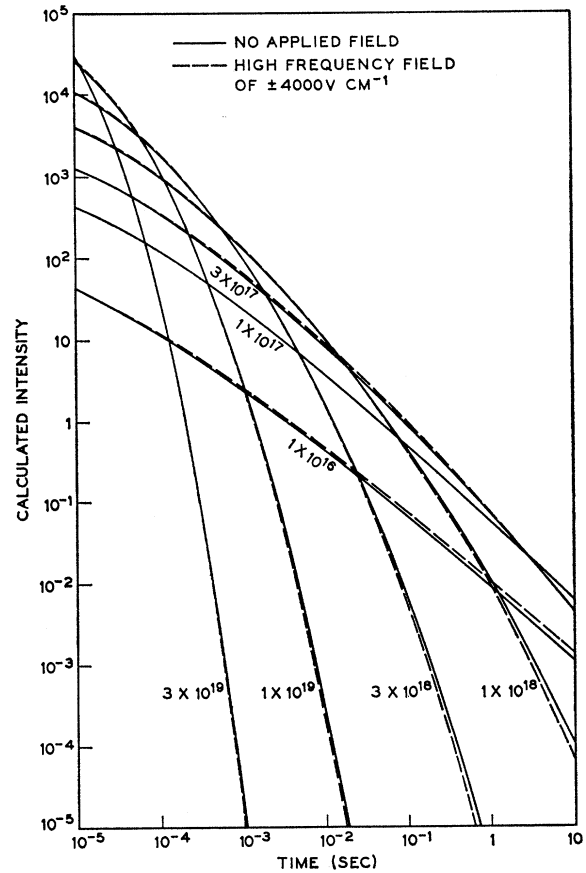

FIG. 4. Calculated luminescent pair-band intensity with and without applied field versus time after photoexcitation. The numbers labeling the curves refer to donor concentrations N_D. $a_h = 14.1$ Å; $a_e < a_h$; D $= 10^6$ sec^{-1}; $N_A = 1$ cm^{-3}.

and $\epsilon=10.18$.[21] Figure 3 shows the time decay of the total pair-band emission for various crystals all containing S-Si pairs but of different concentrations. The concentrations as determined from Hall measurements are given in Table I. The last cloumn of this table also shows the relative intensities of equal size crystals under the same HB-200 mercury arc dc photoexcitation. Figure 4 shows computer solutions of Eq. (12) with $W(R)$ given by Eq. (7) for no field and Eq. (34) for an applied field. The parameters chosen were $D=10^6$ sec^{-1}, and $a_h=14.1$ Å. By Eq. (4) the value chosen for the effective Bohr radius a_h corresponds to an acceptor binding energy of $E_A=0.05$ eV. This energy is in agreement with independent experimental evidence: From Hall measurements on the n-type samples listed in Table I, $E_D=0.09\pm0.02$ eV, and from spectroscopic evidence[14] $E_A+E_D=0.140\pm0.007$ eV. The value of D was chosen to give a good fit to the data from crystal No. 1. The effect of varying D is shown in Fig. 5, together with the experimental curve for crystal No. 1.

B. The Effects of an Applied Electric Field

Figure 6 shows the spectra in the presence and absence of an applied field for sample No. 2 at various times after photoexcitation. Three effects may be
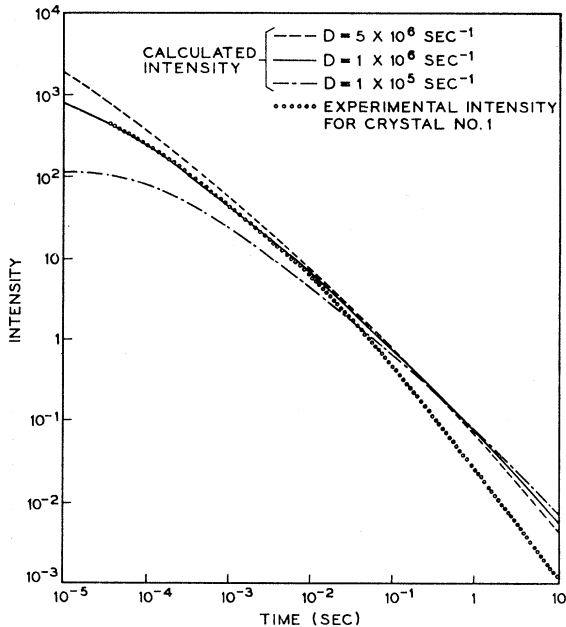
FIG. 5. The effect of varying the parameter D on the calculated decay curves (no applied field), and comparison with the experimental curve for crystal No. 1. Other parameters in the calculation were $N_D=2\times10^{17}$ cm^{-3} and $a_h=14.1$ Å. The experimental curve was shifted vertically (intensity axis) to overlap with the theoretical curve.

[21] D. A. Kleinman and W. G. Spitzer, Phys. Rev. **118**, 110 (1960).

noted: The half-width is increased, the peak position is shifted, and the intensity is changed. The last phenomena is believed to be associated with a change in recombination kinetics through a change in the hole-electron wave function. In Fig. 6 the total intensity of the pair-band is increased in the presence of an electric field before, during, and after excitation. However, in Fig. 7 it may be seen that the intensity may increase, decrease, or not change at all, depending on the impurity concentration and the time after excitation at which the measurement is made. This is in qualitative agreement with the calculations shown in Fig. 4, which
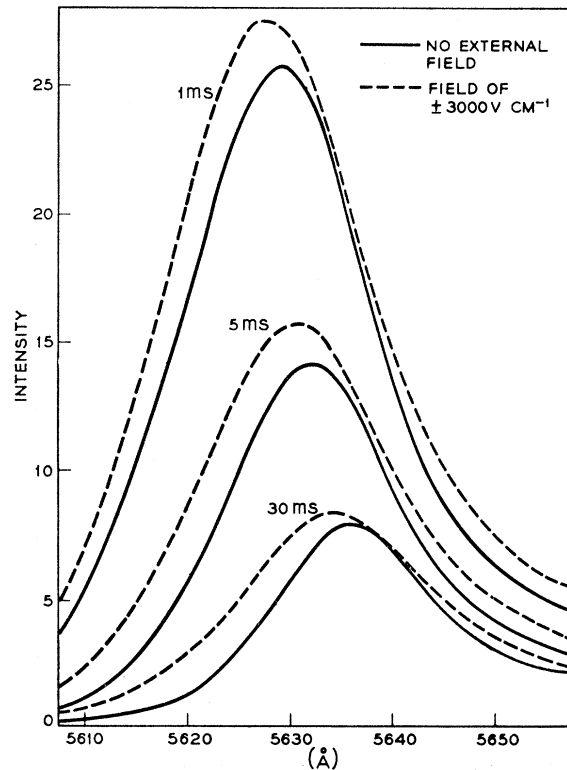
FIG. 6. Pair-band emission spectra, with and without applied high-frequency field for crystal No. 2 at various times (in milliseconds) after photoexcitation. The luminescence was detected for a $3\frac{1}{2}$-msec time interval following the times marked on the diagram.

give at about 0.1 sec after excitation field enhancement of the luminescence by about 20–40% for lightly doped samples (10^{16} cm^{-3}), quenching by about the same amount for more heavily doped samples (3×10^{18}), and nearly no change for intermediate doping.

In the presence of a high-frequency electric field the half-width of the pair band increased in all samples investigated, as illustrated in Fig. 6. By changing the impurity concentration or the time after excitation at which the spectrum is taken one may look at different mean hole-electron separations responsible for the emitted light. Figure 8 shows the change in half-width

produced by a square wave of ±3000 V cm⁻¹ as a function of the mean electron-hole separation responsible for the light. The latter was determined from the experimental peak position of the light by means of Eq. (1). The scatter in points may result mainly from an uncertainty in determining the correct mean electron-hole separation, since the light emission is believed to be partly broadened by phonon cooperatoin rather than the Coulomb term in Eq. (1) alone. However, the experimental points may be seen to be in rather good agreement with the theoretical estimate (dotted line) Eq. (14). For a given crystal a given time after photo-excitation the width of the pair-band emission was found to increase linearly with field provided the frequency of the applied square wave was high enough to avoid electrostatic shielding of the external field due to the crystal conductivity. This meant a frequency of about 1 kc/sec at 50 msec after photoexcitation and 10 kc/sec at 0.5 msec after photoexcitation. However,

FIG. 8. Change in half-width of the pair-band luminescence by an electric field of ±3000 V cm⁻¹ (square wave) as a function of the calculated mean hole-electron separation responsible for the emission. The dashed line gives the theoretical prediction.

frequency field, the field was on before, during, and after excitation. However, during excitation and possibly at short times (microseconds) after, the photoconductivity was probably high enough to allow partial or complete electrostatic shielding even for the maximum frequencies for which a good square wave could be applied (40 kc/sec). This may be part of the reason a detailed quantitative agreement with the calculations in Fig. 4 was not achieved.

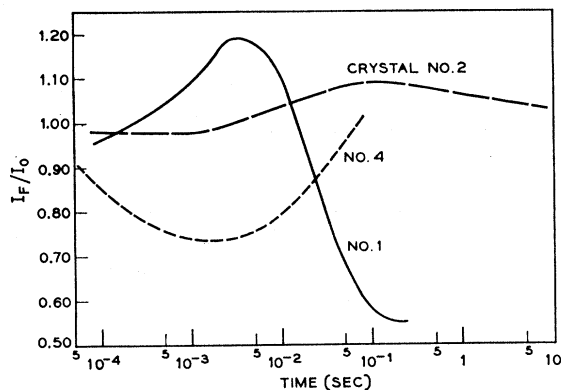A better way of testing the theory for the time decay

FIG. 7. Intensity ratio of the pair-band luminescence with and without an applied electric field versus time after photoexcitation. The field strength was ±4000 V cm⁻¹ (square wave) and changed sign at a frequency of 20 kc/sec.

these numbers depend both on the excitation intensity and on the impurity concentration. The effect of frequency is shown in Fig. 9, which shows oscilloscope tracings giving the light output as a function of time for crystal No. 1 in the absence and presence of a field of varying frequency. At frequencies larger or equal to 2000 cps no electrostatic shielding occurs at 50 msec after photoexcitation, with the result that no change in the luminescence will occur if the frequency is further increased. At 1000 cps the electrostatic shielding just starts to appear and becomes stronger with lower frequencies, until at 20 cps only spikes occur whenever the field direction changes [Fig. 9(e)].

Independent of whether the high-frequency field effect is a quenching or enhancement of the luminescence, the low-frequency spikes always represent an increase in intensity at that time. In determining the experimental curves (Fig. 7) for the ratio of the pair-band intensity with and without an applied high-
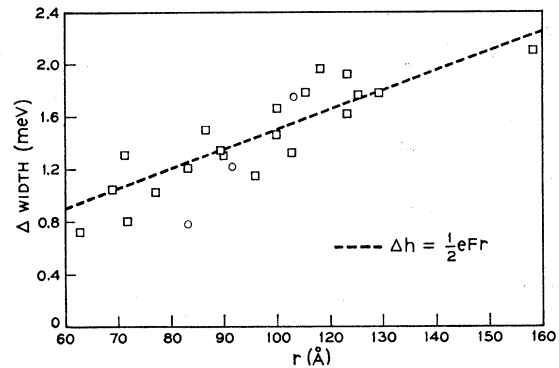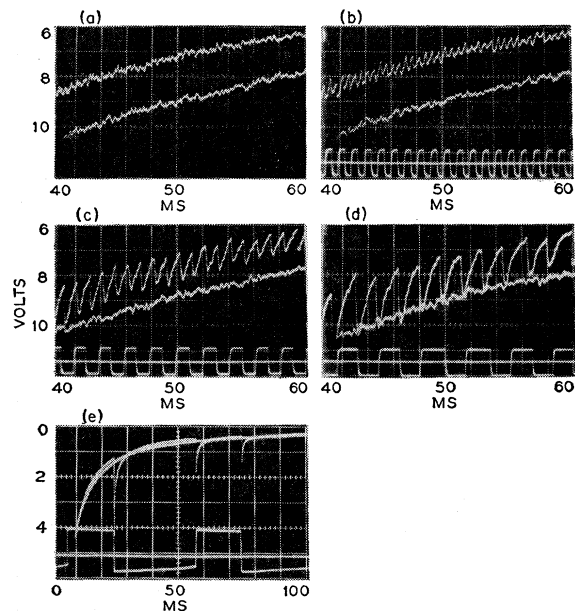

FIG. 9. Pair-band luminescent intensities for crystal No. 1 in the absence and presence of an electric field of ±4000 V cm⁻¹ (square wave) versus time (in milliseconds) after photoexcitation. The field changed sign at a frequency of (a) 4000, (b) 1000, (c) 500, (d) 300, and (e) 20 cps. On all 5 tracings no light emission corresponds to the zero of the vertical scale. The higher intensity, smoother curve, corresponds to no applied field. On (b), (c), (d), and (e) the wave shape of the applied field has been displayed as well.

in the presence of an electric field is to turn the field suddenly on at a certain time after photoexcitation. The ratio of the total light output at this time (spike plus background) to the light output in the absence of a field, should be proportional to the ratio of electron-hole reaction rates, given by Eq. (35). Figure 10 is a drawing of an oscilloscope tracing showing the light decay in the absence of an applied field (dotted curve) and the decay when a voltage resulting in a field of 8000 V cm^{-1} is suddenly applied 10 msec after photoexcitation, and switched off again 23.6 msec later. Both on switching the field on and off, the light output increases suddenly, decays back to the no-field light level, undershoots it, and then finally comes back to the light that would have existed if no field had ever been applied. The sharply increased light output is simply thought to reflect $\langle \Delta W \rangle$. The rather fast decay of the spike is believed to be due to electrostatic shielding, and the undershoot is caused by the fact that certain separation pairs have recombined faster than they would have in the absence of a field. A similar situation exists when the field is switched off. The internal field is then provided by the charge which had previously accumulated to provide the electrostatic screening.

The spikes appearing on application of a field of 8000 V cm^{-1} were investigated by plotting the log of the intensity increase (over the no-field intensity) against the time after field application. A typical plot of this nature is shown in Fig. 11. Extrapolating to zero time, a number proportional to $\langle \Delta W \rangle$ is obtained. Taking from Fig. 10 the intensity proportional to W_0 at the time the field was applied one obtains $\langle W_F \rangle / W_0$. By applying the voltage at different times after photoexcitation and converting from time to mean electron-hole spacing, using Fig. 2, one may obtain $\langle W_F \rangle / W_0$ as a function of the mean electron-hole spacing r. The experimental points have been plotted in Fig. 12 together with the calculated values (solid line) using Eq. (35).
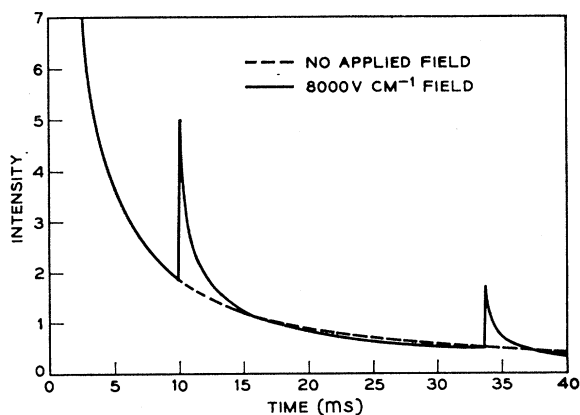

FIG. 10. Pair-band luminescence versus time (in milliseconds) after photoexcitation with no field, and an 8000 V cm^{-1} dc field turned on at 10 msec and turned off at 33.6 msec after photoexcitation for crystal No. 1.
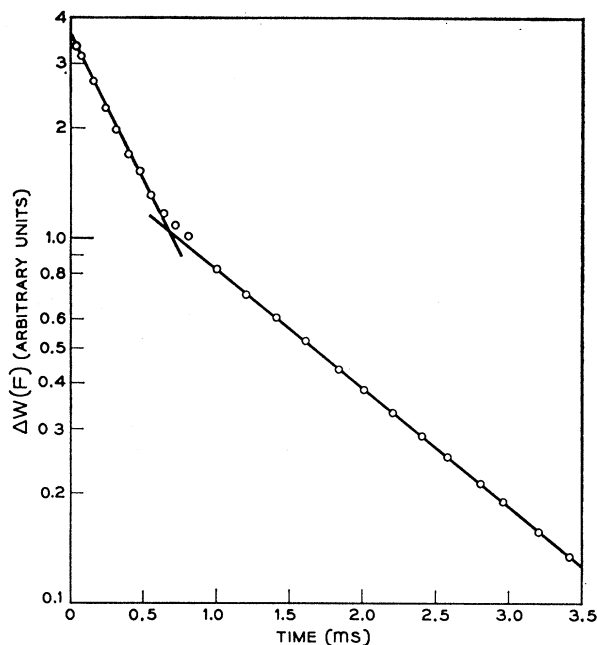

FIG. 11. The change in light emission $\langle \Delta W \rangle$, produced in crystal No. 1 by application of an 8000 V cm^{-1} step-function field applied 10 msec after photoexcitation. The time axis (milliseconds) has its zero at field application.

Figure 13 shows the increase in the reaction rate $\langle \Delta W \rangle = \langle W_F \rangle - W_0$ as a function of the applied field at a fixed time after photoexcitation. The full line was calculated by using Eq. (36).

In the present experimental arrangements with fields up to 12 000 V cm^{-1} (ac or dc), the crystals showed no electroluminescence in the absence of photoexcitation.

VI. SUMMARY AND CONCLUSIONS

Four electrophotoluminescent effects (Gudden-Pohl effect, field quenching, enhancement, and broadening) have been observed in the low-temperature green-edge emission in previously excited GaP. All four effects can be explained semiquantitatively by a model which attributes the luminescence to the reaction of an electron bound to a donor impurity (sulfur) with a hole bound to an acceptor impurity (silicon). The nature of the impurities was established by independent evidence.[14]

The impurity wave functions were approximated by hydrogenic wave functions, with Bohr radii obtained from the experimental impurity binding energies. The luminescent decay kinetics is calculated on the assumption of a random distribution of impurities.[13] A nonexponential time decay of the luminescence can thus be explained without invoking a continuous distribution of traps[22] of unknown origin. The electric-field effects enter the theory through the action of the field

---

[22] J. T. Randall and M. H. F. Wilkins, Proc. Roy. Soc. (London) A184, 390 (1945).

on the impurity wave functions, using the WKB approximation. In the presence of an applied electric field before, during, and after photoexcitation, the theory predicts field enhancement of the total light at short times, and quenching at long times after photoexcitation. The crossover point between enhancement and quenching shifts to longer times for lower impurity concentrations, and shorter times for higher concentrations. Gudden-Pohl spikes are observed on application and removal of a dc electric field, and on polarity reversal of a slowly alternating ac field. The relative height of these spikes are approximately accounted for by the increased electron-hole reaction rates in the presence of an applied electric field. The spectral width of the emission at a given time after photoexcitation is broadened, due to the electric field, by an amount which is in quantitative agreement with the mean dipole energy of the donor-acceptor pairs responsible for the luminescence.

The quantitative agreement between theory and experiment is as good as can be expected for the simple theoretical model employed. Some of the disagreement, observed in Figs. 12 and 13, between theory and experiment at large separations and large fields, results from the fact that the expansions made in deriving Eq. (33) reach the limit of applicability. Some dis-

FIG. 13. The change in light emission $\langle \Delta W \rangle$ produced in crystal No. 1 by application of a field step function versus the strength of the applied dc field. The field was applied 10 msec after photoexcitation. The mean electron-hole separation responsible for this emission is 87 Å (see Fig. 2).

agreement is believed to result from the simplicity of the theoretical model employed. A more sophisticated theoretical model would avoid:

(a) The use of simple hydrogenic wave functions.

(b) The assumptions, in deriving Eq. (11), that the donor concentration is "much larger" than the acceptor concentration, and that in considering one acceptor the influence of neighboring acceptors may be neglected. At a concentration of 10^{18} cm^{-3} with a random distribution, this will be no longer true.[23]

(c) The neglect of the influence of local electric fields, resulting from the ionized donors and acceptors which are present after the first electron-hole reactions have taken place. These fields are of considerable size,[23] and may be expected to alter the kinetics of electron-hole reaction rates appreciably.

(d) The neglect of the donor-acceptor interaction. This will tend to move the maximum of the hole-electron overlap slightly away from the donor site towards the acceptor.

One would expect that the mechanism of bound hole-bound electron reaction discussed in this paper should be quite common in semiconductors and may explain much previously published and often poorly understood data on the subjects of photoluminescence and electrophotoluminescence. It was often realized in relevant
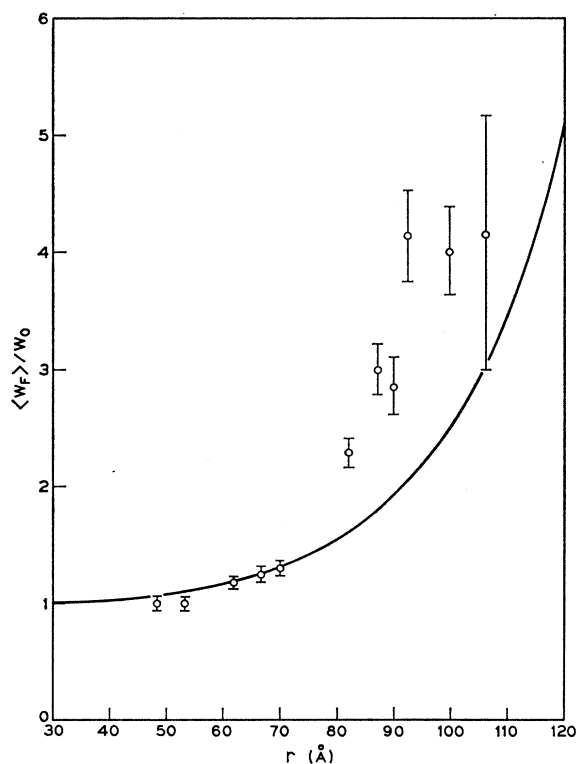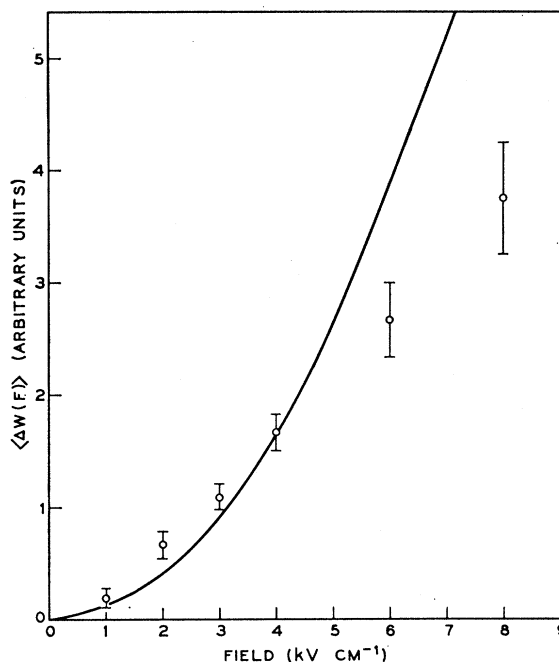

FIG. 12. The experimental and theoretical (full-line) ratio of $\langle W_F \rangle / W_0$ for crystal No. 1 versus electron-hole separation of the pairs responsible for the light emission. The theoretical curve was calculated with $a_h = 14.1$ Å, $E_A = 0.05$ eV, and $F = 8000$ V cm^{-1}.

[23] K. Colbow, Can. J. Phys. 41, 1801 (1963).

previous work[7] that the "coactivator" is frequently as important as the "activator." However, the experimental situation was usually sufficiently different to make the definite exclusion of alternative explanations impossible at this stage.

APPENDIX I: INDIRECT TRANSITIONS BETWEEN IMPURITIES

The matrix element $H_{13}(\sigma)$ for an indirect transition from state 1 to 3 with emission of a single phonon of momentum $\mathbf{K}+\sigma$, where $\mathbf{K}$ is the minimum separation, and emission of a photon is given by

$$H_{13}(\sigma)=\left[\sum_2 \langle\varphi_1|p|\varphi_2\rangle\langle\varphi_2|H_{\mathrm{ph}}|\varphi_3\rangle(E_1-E_2)^{-1}\right.$$
$$\left.+\langle\varphi_1|H_{\mathrm{ph}}|\varphi_2\rangle\langle\varphi_2|p|\varphi_3\rangle(E_1-E_2)^{-1}\right], \quad (37)$$

where C contains parameters irrelevant to the present argument, p is the momentum operator, and H_{ph} is the phonon operator. The sum is over all intermediate states φ_2.

If the energy denominators (E_1-E_2) are large compared to the Coulomb effects of the impurities on any excited states it will be a good approximation to replace the φ_2 by Bloch states $\psi_{n_2}(\mathbf{k},\mathbf{r})$.

We also write the impurity states φ_1,φ_3 as a superposition of Bloch states:

$$\varphi_1(\mathbf{r})=\sum_k A_1(\mathbf{k})\psi_{n_1}(\mathbf{k},\mathbf{r}),$$

$$\varphi_3(\mathbf{r})=\sum_k A_3(\mathbf{k}')\psi_{n_3}(\mathbf{k}',\mathbf{r}), \quad (38)$$

where $\mathbf{k}'=\mathbf{k}+\mathbf{K}+\sigma$, and we are considering only

phonon emission. Substituting in Eq. (37), one obtains

$$H_{13}(\sigma)=C\sum_{n_2,k}{}' A_1{}^*(\mathbf{k})A_3(\mathbf{k}')M, \quad (39)$$

$$M\equiv\frac{\langle\psi_{n_1}(\mathbf{k},\mathbf{r})|p|\psi_{n_2}(\mathbf{k},\mathbf{r})\rangle}{E_1-E_{n_2}(\mathbf{k})}$$
$$\times\langle\psi_{n_2}(\mathbf{k},\mathbf{r})|H_{\mathrm{ph}}|\psi_{n_3}(\mathbf{k}',\mathbf{r})\rangle$$
$$+\frac{\langle\psi_{n_1}(\mathbf{k},\mathbf{r})|H_{\mathrm{ph}}|\psi_{n_2}(\mathbf{k}',\mathbf{r})\rangle}{E_1-E_{n_2}(\mathbf{k}')}$$
$$\times\langle\psi_{n_2}(\mathbf{k}',\mathbf{r})|p|\psi_{n_3}(\mathbf{k}',\mathbf{r})\rangle. \quad (40)$$

If the impurities have large spread in real space, and hence small spread in k space, the dependence of M on k may be neglected. Hence one may write

$$H_{13}(\sigma)=C\{\sum_k A_1{}^*(\mathbf{k})A_3(\mathbf{k}')\}\sum_{n_2} M_0. \quad (41)$$

M_0 is obtained from Eq. (40) by replacing $\mathbf{k}$ by $\mathbf{k}_{0_1}$, and $\mathbf{k}'$ by $\mathbf{k}_{0_3}$, where $\mathbf{k}_{0_3}=\mathbf{k}_{0_1}+\mathbf{K}$. Writing

$$\varphi_1=\psi_e(\mathbf{r})[e^{i\mathbf{k}_{0_1}\cdot\mathbf{r}}u_{n_1}(\mathbf{k}_{0_1},\mathbf{r})],$$
$$\varphi_3=\psi_h(\mathbf{r})[e^{i\mathbf{k}_{0_3}\cdot\mathbf{r}}u_{n_3}(\mathbf{k}_{0_3},\mathbf{r})], \quad (42)$$

where $\psi_e(\mathbf{r})$ and $\psi_h(\mathbf{r})$ are "envelope functions" given by the transform of $A_1(\mathbf{k})$ and $A_3(\mathbf{k})$, respectively, one finds

$$\sum_k A_1{}^*(\mathbf{k})A_3(\mathbf{k}')=\int\psi_e{}^*(\mathbf{r})\psi_h(\mathbf{r})e^{-i\sigma\cdot\mathbf{r}}d\mathbf{r}. \quad (43)$$

The overlap integral in Eq. (43) will be a maximum for small σ usually, that is, for σ smaller or of the order of the larger k spread in $\psi_e(\mathbf{r})$ or $\psi_h(\mathbf{r})$. For larger σ the integral will decrease rapidly. Thus in order to calculate the transition probability

$$W=(2\pi/\hbar)\sum_\sigma \delta(E_1-E_3-\hbar\omega_{\mathrm{photon}}-\hbar\omega_{\mathrm{phonon}})|H_{13}(\sigma)|^2 \quad (44)$$

in a very crude manner, one may approximate Eq. (44) by replacing $H_{13}(\sigma)$ by $H_{13}(0)$, and use as a cutoff for the σ summation the reciprocal Bohr radius of the more tightly bound of the envelope functions $\psi_e(r)$, $\psi_h(r)$.
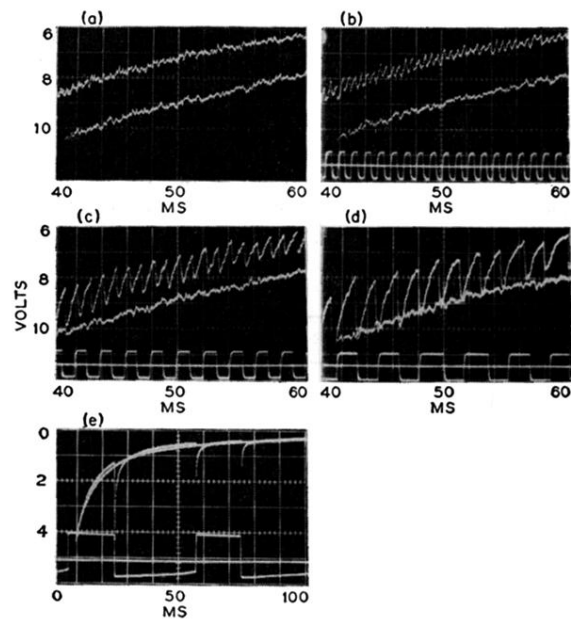
FIG. 9. Pair-band luminescent intensities for crystal No. 1 in the absence and presence of an electric field of ± 4000 V cm^{-1} (square wave) versus time (in milliseconds) after photoexcitation. The field changed sign at a frequency of (a) 4000, (b) 1000, (c) 500, (d) 300, and (e) 20 cps. On all 5 tracings no light emission corresponds to the zero of the vertical scale. The higher intensity, smoother curve, corresponds to no applied field. On (b), (c), (d), and (e) the wave shape of the applied field has been displayed as well.